ChemComm

COMMUNICATION

View Article Online
View Journal | View Issue

Cite this: *Chem. Commun.*, 2023, 59, 7591

Received 28th April 2023,
Accepted 23rd May 2023

DOI: 10.1039/d3cc02056h

rsc.li/chemcomm

Development of light-induced disruptive liposomes (LiDL) as a photoswitchable carrier for intracellular substance delivery†

Taichi Tsuneishi,[a] Keiichi Kojima,[ab] Fumika Kubota,[c] Hideyoshi Harashima,[c] Yuma Yamada[c] and Yuki Sudo[*ab]

Light-driven inward proton pump rhodopsin *Rm*XeR was embedded in pH-sensitive liposomes. Substance release from the proteoliposomes was observed following light illumination both *in vitro* and in cells, indicating the successful production of light-induced disruptive liposomes (LiDL). Thus, LiDL is a photoswitchable carrier utilized for intracellular substance delivery.

Artificial lipid bilayer vesicle liposomes consist of hydrophobic and hydrophilic molecules such as triglycerides, phospholipids and sterols, and any molecules including chemicals and drugs can be incorporated into those liposomes. The characteristics of liposomes allow them to be used as carriers for intracellular substance delivery.[1] It should be noted that liposomes need to have contradictory properties, *i.e.* high and low stability in extracellular and intracellular compartments, respectively. So far, various techniques have been developed and applied to solve that dilemma. The lipid composition affects the stability of liposomes and its optimization enables the production of stable liposomes at various conditions (*e.g.*, high temperature and low pH), which prevents their degradation in the extracellular compartment.[2] In addition, liposomes should have a low stability when they are taken up into cells for efficient intracellular substance delivery. To disrupt liposomes in a condition-dependent manner, several methods have been developed.[3] Among them, pH-sensitive liposomes are utilized so far.[4,5] For instance, liposomes consisting of 1,2-dioleoyl-*sn*-glycero-3-phosphoethanolamine (DOPE) and cholesteryl hemisuccinate (CHEMS) have been established as a method for disrupting the liposome structure in cells due to the phase separation of the DOPE/CHEMS lipid bilayer at an acidic pH (below 5.5) in endosomes, which leads to the release of their contents into the cells (Fig. S1, ESI†).[6] In this study, we focused on light as a stimulus having a high spatiotemporal resolution to achieve a more precise release of the contents from pH-sensitive liposomes. To initiate acidification inside liposomes with light, we employed *Rm*XeR (Fig. 1A). *Rm*XeR was identified from a marine bacterium *Rubricoccus marinus* and phylogenetically categorized into Xenorhodopsin (XeR) functioning as an inward proton pump.[7] Microbial rhodopsins, including *Rm*XeR, are membrane-embedded photoreceptor proteins having vitamin-A aldehyde retinal as a chromophore and they show light-dependent molecular functions such as ion transport and signal transduction.[8] Among them, *Rm*XeR pumps protons (H^+) from the extracellular side to the intracellular side and induces

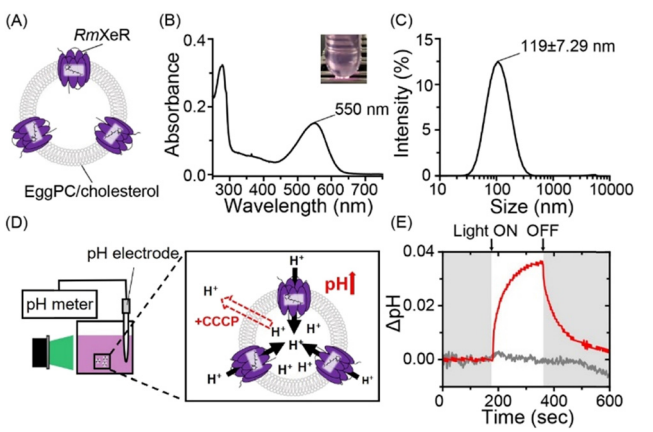

Fig. 1 Incorporation of *Rm*XeR into a lipid bilayer consisting of EggPC/cholesterol. (A) Schematic of pH-insensitive liposomes containing *Rm*XeR. (B) Absorption spectrum of the proteoliposome with its visible color (inset). (C) Hydrodynamic diameter measured by DLS. (D) Schematic of the measurement of light-induced pH changes in the solution. (E) Light-induced pH change with (gray) or without (red) the proton-selective ionophore, CCCP.

[a] *Graduate School of Medicine, Dentistry and Pharmaceutical Sciences, Okayama University, Okayama, 700-8530, Japan. E-mail: sudo@okayama-u.ac.jp*
[b] *Faculty of Medicine, Dentistry and Pharmaceutical Sciences, Okayama University, Okayama, 700-8530, Japan*
[c] *Faculty of Pharmaceutical Sciences, Hokkaido University, Sapporo, 060-0812, Japan*

† Electronic supplementary information (ESI) available. See DOI: https://doi.org/10.1039/d3cc02056h

intracellular acidification.[7] In fact, a large increase in pH (approximately 0.1 unit) was observed for *E. coli* cells heterologously expressing *Rm*XeR.[7] This means that *Rm*XeR can be an effective tool for facilitating the disruption of pH-sensitive liposomes with light. In this study, we established light-induced disruptive liposomes (LiDL), and used them as a carrier for intracellular substance delivery.

Firstly, liposomes consisting of Egg yolk phosphatidylcholine (EggPC) and cholesterol at a 7 : 3 molar ratio were prepared using the lipid hydration method,[9] as a model for pH-insensitive liposomes, where purified *Rm*XeR was incorporated into liposomes using the dilution method (Fig. 1A).[10] As seen in Fig. 1B, the sample showed a purple color corresponding to visible absorption around 550 nm. This value is almost identical to that of *Rm*XeR in *n*-dodecyl-β-D-maltoside (DDM) detergent micelles reported previously (*i.e.*, 550 nm),[7] indicating the successful production of the desired proteoliposomes shown in Fig. 1A. The size and distribution of those proteoliposomes were estimated by dynamic light scattering (DLS) measurements as 119 ± 7.29 nm and monodispersity (polydispersity index (PdI) = 0.20 ± 0.019), respectively (Fig. 1C and Table S1, ESI†). We then tested the inward proton pump activity of those proteoliposomes by monitoring the environmental pH in a solution containing 100 mM NaCl. The sample was illuminated with green light (550 ± 10 nm) for 3 min at an intensity of 0.080 mW mm^{-2}, as schematically presented in Fig. 1D. The pH was increased approximately 0.035 units, and the changes in pH slowly returned to around the initial value after stopping the light (red line in Fig. 1E). The increase in pH was not observed for that sample in the presence of the protonophore carbonyl cyanide 3-chlorophenylhydrazone (CCCP) (gray line in Fig. 1E), indicating the light-driven inward proton transport activity of *Rm*XeR in the proteoliposomes. We had confirmed the linearity between the initial slope amplitude and the light intensity below 0.14 mW mm^{-2} previously,[7] indicating that these experiments are quantitative. Thus, we successfully prepared proteoliposomes, which could induce acidification within them upon light illumination. The results also allowed us to estimate the changes in pH value inside the proteoliposomes from the size of the proteoliposomes (*i.e.*, 120 nm). For estimation, several parameters were used as follows; surface area of the lipid bilayer (outer lipid bilayer; 74 × 10^{-20} m^2 and inner lipid bilayer; 61 × 10^{-20} m^2 for EggPC), thickness (37 × 10^{-10} m for EggPC),[11] surface area of cholesterol in the hydrated dipalmitoyl phosphatidylcholine (DPPC) bilayers containing 25–40% cholesterol (27 × 10^{-20} m^2)[12] and the size of the bacteriorhodopsin monomer (corresponding to 40 lipid molecules) (Fig. S2, ESI†).[13] Using these parameters, we estimated that the inside of the proteoliposomes was acidified from pH 7.0 to 4.8. It has been previously reported that pH-sensitive liposomes are disrupted below pH 5.5.[6] Therefore, we assumed that proteoliposomes containing *Rm*XeR have enough of a change in pH to disrupt the pH-sensitive liposomes.

Secondly, we added the pH-sensitivity into the proteoliposomes. Liposomes consisting of DOPE and CHEMS at a 7 : 3 molar ratio were prepared by the lipid hydration method[9]

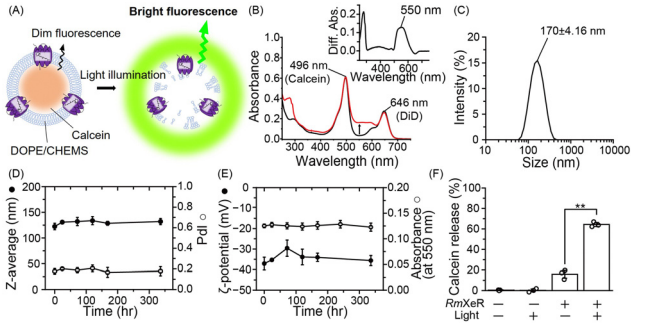

Fig. 2 Production of LiDL and its physicochemical properties. (A) Schematic of calcein-encapsulated pH-sensitive liposomes containing *Rm*XeR. (B) Absorption spectra of proteoliposomes. Black and red lines show the absorption spectra before and after incorporation of *Rm*XeR, respectively. The inset shows the difference absorption spectrum. (C) Hydrodynamic diameter of LiDL. (D) Size (*Z*-average, closed circles) and polydispersity index (PdI, open circles) at 4 °C (n = 3). (E) ζ-Potential (closed circles) and absorbance of *Rm*XeR at 550 nm in LiDL (open circles) at 4 °C (n = 3). (F) Calcein release from liposomes with or without *Rm*XeR and light illumination (n = 3). Error bars represent the standard deviation. Asterisks indicate significant differences from the value of LiDL without light illumination (**p < 0.01; Student's t test).

as a model for pH-sensitive liposomes, in which the fluorescence probe calcein was incorporated into the liposomes. Calcein is a water soluble fluorescent dye that has a self-quenching property at high concentrations and emits bright fluorescence upon dilution. Purified *Rm*XeR was incorporated into calcein-encapsulated liposomes by the dilution method (Fig. 2A).[10] We expected that those proteoliposomes would be disrupted by green light illumination due to the phase separation of the DOPE/CHEMS lipid bilayer at an acidic pH, as schematically shown in Fig. 2A. The absorption spectra of proteoliposomes showed an increase in absorbance around 550 nm compared with liposomes without *Rm*XeR and their difference absorption spectra showed a peak around 550 nm (Fig. 2B), indicating the successful production of the desired proteoliposomes. The size and distribution of the proteoliposomes were estimated as 170 ± 4.16 nm and monodispersity (polydispersity index (PdI) = 0.15 ± 0.019), respectively (Fig. 2C and Table S1, ESI†). Because a suitable size (*i.e.*, 50–200 nm) and monodispersity of liposomes is essential for their efficient incorporation into living cells,[14] the constructed proteoliposomes are expected to be suitable for cellular delivery. In addition, for intracellular substance delivery, liposomes should have a high stability against stimuli such as heat. Thus, we examined the stability of those proteoliposomes. As expected, the physicochemical properties (size, PdI, ζ-potential and absorbance of *Rm*XeR at 550 nm) were almost constant for 2 weeks at 4 °C (Fig. 2D and E), indicating the high stability of those proteoliposomes.

Next, we tested whether the proteoliposomes were disrupted by green light illumination by measuring the fluorescence of calcein. As seen in Fig. 2F, the calcein release ratio was estimated as 64.3 ± 1.97% for proteoliposomes exposed to green light, a value that was significantly larger than that without green light illumination (16 ± 3.7%) and of liposomes alone with or without green light illumination (0.4 ± 0.3% and

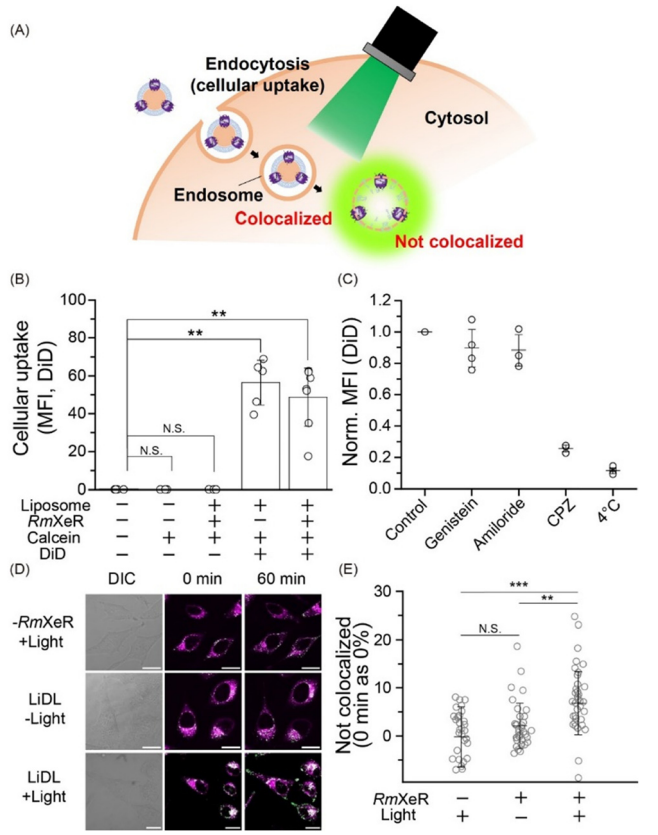

Fig. 3 Applicability of LiDL as a carrier for intracellular substance delivery in HeLa cells. (A) Schematic of LiDL as a carrier for calcein in HeLa cells. (B) Cellular uptake of LiDL evaluated by flow cytometry as mean fluorescence intensity (MFI). Error bars represent the standard deviation and asterisks indicate significant differences from the value without the addition of liposomes (N.S.; not significant, $p > 0.05$, $^{**}p < 0.01$; Dunnett's test, n = 3–6). (C) Evaluation of the cellular uptake pathway of LiDL by endocytosis inhibitors. (D) CLSM images of HeLa cells after the uptake of liposomes at room temperature. DIC (differential interference contrast) and fluorescence images before and after green light illumination for 60 min are shown. Scale bars indicate 20 μm. (E) Quantitative analysis of the rate of colocalization. n = 33–47 cells were independently examined 3–4 times. Error bars represent the standard deviation. Asterisks indicate significant differences (N.S.; not significant, $p > 0.05$, $^{**}p < 0.01$, $^{***}p < 0.001$; Scheffe's test).

0.2 ± 1.4%, respectively). These results implied that calcein was released from the proteoliposomes in a light-dependent manner. Thus, we succeeded in producing proteoliposomes that could be disrupted by light, and named them light-induced disruptive liposomes (LiDLs).

Thirdly, we incorporated LiDL into mammalian HeLa cells to evaluate them as a carrier for intracellular substance delivery (Fig. 3A). To evaluate cellular uptake, LiDL was labeled with 1,1′-dioctadecyl-3,3,3′,3′-tetramethylindodicarbocyanine (DiD), which is a lipophilic carbocyanine dye showing red fluorescence that is used to label the lipid bilayer. The cellular uptake was monitored by measuring the change in fluorescence intensity of DiD after 1 h incubation at 37 °C. The results show that liposomes with or without *Rm*XeR showed a significantly larger cellular uptake than the controls (*i.e.* without liposomes, calcein alone and LiDL without DiD) (Fig. 3B). Similar results were also observed by confocal laser scanning microscopy (CLSM) (Fig. S3, ESI†). These results implied that LiDL effectively entered HeLa cells. It is well-known that cellular uptake is achieved by several endocytosis mechanisms, including clathrin-dependent endocytosis, caveolae-dependent endocytosis, fast endophilin-mediated endocytosis (FEME), macropinocytosis and phagocytosis.[15] Thus, we explored the pathway of cellular uptake of LiDL using endocytosis inhibitors, genistein for caveolae-dependent endocytosis,[16] amiloride for macropinocytosis[17] and chlorpromazine (CPZ) for clathrin-dependent endocytosis.[18] Observations at low temperature (4 °C) were also performed as a control for the inhibition of all cellular uptake mechanisms. As seen, the cellular uptake of LiDL was significantly impaired by the addition of CPZ (approx. 25% compared with the control), but not by the addition of genistein or amiloride (89% and 97%, respectively) (Fig. 3C). Similar results were also observed by CLSM (Fig. S4, ESI†). These results suggested that LiDL is mainly taken up into HeLa cells *via* clathrin-dependent endocytosis.

When the substances were incorporated into the cells, some of them were decomposed in lysosomes, leading to the reduction of their biochemical activities. Therefore, the incorporated substances should escape from immature endosomes (called endosome escape) for efficient intracellular substance delivery.[19] Then, to monitor the light-dependent endosome escape, green light (approx. 559 nm) was applied to HeLa cells for 60 min at 4.3 W mm^{-2} and changes in the localization of calcein and endosomes (lysosomes) were observed by using a fluorescence marker lysotracker. Before the light illumination (*i.e.*, 0 min), all samples (liposomes alone with light [−*Rm*XeR/+light] and LiDL with or without light [LiDL/+light] and [LiDL/−light], respectively) showed white signals corresponding to the colocalization of calcein and endosomes (Fig. 3D). The white signals were also observed after 60 min incubation both for [−*Rm*XeR/+light] and [LiDL/−light]. On the other hand, green fluorescence signals originating from calcein were observed for [LiDL/+light] after 60 min incubation, suggesting intracellular calcein release (*i.e.*, endosome escape).

To quantitatively evaluate the calcein release, we calculated the value of "Not colocalized (%)" by using the Mander coefficient, which is a colocalization indicator for dual-color imaging (see ESI†).[20] The values of "not colocalized (%)" were around zero both for liposomes alone with light (−0.153 ± 6.20%) and LiDL without light (1.28 ± 6.34%) (Fig. 3E), while it was significantly increased in LiDL with light (6.80 ± 6.54%), suggesting intracellular calcein release (Fig. 3E). Thus, we concluded that the LiDL developed in this study are effective carriers for intracellular substance delivery.

Fourth, we added stearyl octaarginine (STR-R8, 8.5 mol% of lipids), which is a positively charged cell-penetrating peptide,[21] into LiDL to improve their intracellular delivery efficiency (Fig. 4A). As a model for the intracellular delivery of substances, a mRNA encoding EGFP was also incorporated into the liposomes by the ethanol dilution method[22] after which *Rm*XeR was incorporated into liposomes by the dilution method.[10]

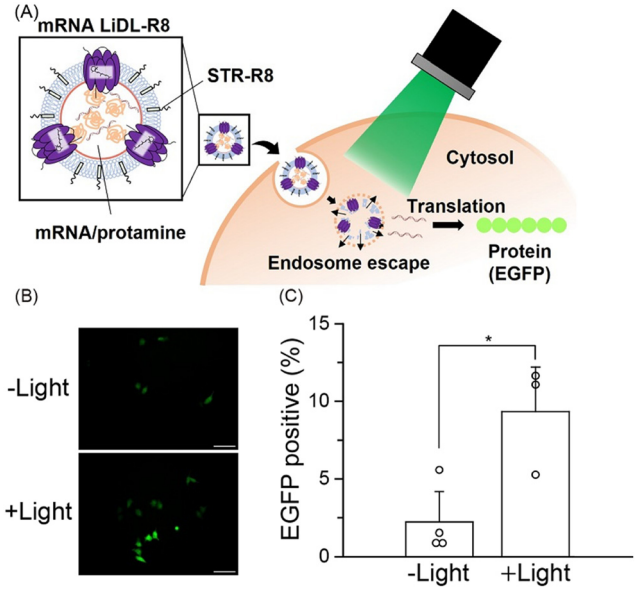

Fig. 4 Light-induced mRNA delivery by LiDL. (A) Schematic of mRNA delivery in HeLa cells using LiDL. (B) Microscopic fluorescence images of EGFP with or without light illumination. Scale bars indicate 100 μm. (C) Transfection efficacy of LiDL containing a mRNA encoding EGFP with or without light illumination. Error bars represent the standard deviation (n = 3–4). Asterisks indicate significant differences (*$p < 0.05$; Student's t test).

Proteoliposomes containing STR-R8 were named LiDL-R8 (Fig. 4A). As expected, the surface charge of proteoliposomes was changed from a negative value (−49 mV) for LiDL to a positive value (+29 mV) for LiDL-R8, resulting in a significant increase in cellular uptake (Fig. 4A and Fig. S5, ESI†). Using a RiboGreen assay, we measured the mRNA content and estimated its entrapment efficiency as 24 ± 9.4% (2.3 ± 1.1 μg mL^{-1} mRNA). It should be noted that, except for the ζ-potential, the physicochemical properties of LiDL-R8 (*i.e.*, size = 218 ± 23.4 nm and PdI = 0.24 ± 0.074) were almost identical to those of LiDL (size = 210 ± 27.1 nm, PdI = 0.24 ± 0.091), suggesting less effect(s) of STR-R8 on the formation of LiDL (Table S2, ESI†). LiDL-R8 was then added into HeLa cells (60–70% confluent) with and without green light illumination (545 ± 10 nm) for 60 min followed by incubation for 23 hr at 37 °C. As shown in Fig. 4B and C, the fluorescence signal of LiDL-R8 was significantly enhanced from 2.2 ± 2.0% to 9.5 ± 2.7% by green light illumination. These results indicated both the release of mRNA encoding EGFP upon light illumination and the translation that produced EGFP protein in the cells (Fig. 4A). Thus, LiDL is useful for intracellular delivery both of chemicals (*e.g.*, hydrophilic and hydrophobic molecules such as calcein and Nile Red, respectively) and biomolecules (*e.g.*, mRNA). To improve the efficiency of the content release, we will characterize the structure of the formed liposomes using various methods such as electron microscopy and optimize the experimental conditions such as buffer concentration in the future.

In conclusion, we developed light-induced disruptive liposomes (LiDLs) that have a high stability in the dark and demonstrated that they are useful, especially for life scientists as an optically controllable carrier for intracellular substance delivery.

Conflicts of interest

There are no conflicts to declare.

Notes and references

1 K. Maruyama, *Adv. Drug Delivery Rev.*, 2011, **63**, 161–169.
2 M. Taira, N. Chiaramoni, K. Pecuch and S. Alonso-Romanowski, *Drug Delivery*, 2004, **11**, 123–128.
3 A. Scomparin, H. F. Florindo, G. Tiram, E. L. Ferguson and R. Satchi-Fainaro, *Adv. Drug Delivery Rev.*, 2017, **118**, 52–64.
4 Y. Sato, *Chem. Pharm. Bull.*, 2021, **69**, 1141–1159.
5 H. Ding, P. Tan, S. Fu, X. Tian, H. Zhang, X. Ma, Z. Gu and K. Luo, *J. Controlled Release*, 2022, **348**, 206–238.
6 Y. Fan, C. Chen, Y. Huang, F. Zhang and G. Lin, *Colloids Surf., B*, 2017, **151**, 19–25.
7 S. Inoue, S. Yoshizawa, Y. Nakajima, K. Kojima, T. Tsukamoto, T. Kikukawa and Y. Sudo, *Phys. Chem. Chem. Phys.*, 2018, **20**, 3172–3183.
8 O. P. Ernst, D. T. Lodowski, M. Elstner, P. Hegemann, L. S. Brown and H. Kandori, *Chem. Rev.*, 2014, **114**, 126–163.
9 Y. Yamada, H. Akita, H. Kamiya, K. Kogure, T. Yamamoto, Y. Shinohara, K. Yamashita, H. Kobayashi, H. Kikuchi and H. Harashima, *Biochim. Biophys. Acta, Biomembr.*, 1778, **2008**, 423–432.
10 J.-L. Rigaud and D. Lévy, *Methods Enzymol.*, 2003, **372**, 65–86.
11 C. Huang and J. Mason, *Proc. Natl. Acad. Sci. U. S. A.*, 1978, **75**, 308–310.
12 C. Hofsäß, E. Lindahl and O. Edholm, *Biophys. J.*, 2003, **84**, 2192–2206.
13 M. Orwick-Rydmark, J. E. Lovett, A. Graziadei, L. Lindholm, M. R. Hicks and A. Watts, *Nano Lett.*, 2012, **12**, 4687–4692.
14 D. Guimarães, A. Cavaco-Paulo and E. Nogueira, *Int. J. Pharm.*, 2021, **601**, 120571.
15 J. J. Rennick, A. P. Johnston and R. G. Parton, *Nat. Nanotechnol.*, 2021, **16**, 266–276.
16 T. Akiyama, J. Ishida, S. Nakagawa, H. Ogawara, S.-I. Watanabe, N. Itoh, M. Shibuya and Y. Fukami, *J. Biol. Chem.*, 1987, **262**, 5592–5595.
17 T. R. Kleyman and E. J. Cragoe Jr, *J. Membr. Biol.*, 1988, **105**, 1–21.
18 Z. Wang, A. B. Asenjo and D. D. Oprian, *Biochemistry*, 1993, **32**, 2125–2130.
19 J. Rink, E. Ghigo, Y. Kalaidzidis and M. Zerial, *Cell*, 2005, **122**, 735–749.
20 E. Manders, F. Verbeek and J. Aten, *J. Microsc.*, 1993, **169**, 375–382.
21 S. Futaki, W. Ohashi, T. Suzuki, M. Niwa, S. Tanaka, K. Ueda, H. Harashima and Y. Sugiura, *Bioconjugate Chem.*, 2001, **12**, 1005–1011.
22 Y. Yamada, K. Somiya, A. Miyauchi, H. Osaka and H. Harashima, *Sci. Rep.*, 2020, **10**, 1–13.